Front. Struct. Civ. Eng. 2023, 17(4): 566–583
https://doi.org/10.1007/s11709-023-0905-x

RESEARCH ARTICLE

Undrained seismic bearing capacity of strip footing adjacent to a heterogeneous excavation

Ramin VALI[a*], Saeed KHOSRAVI[b], Majid BEYGI[c]

[a] *Department of Civil Engineering, Technical and Vocational University, Tehran 1435761137, Iran*
[b] *Department of Mining Engineering, Shahid Bahonar University of Kerman, Kerman 7616913439, Iran*
[c] *Department of Civil Engineering, Yazd University, Yazd 8915818411, Iran*
[*] *Corresponding author. E-mail: rvali@tvu.ac.ir*

ABSTRACT The analysis of the bearing capacity of strip footings sited near an excavation is critical in geotechnics. In this study, the effects of the geometrical features of the excavation and the soil strength properties on the seismic bearing capacity of a strip footing resting on an excavation were evaluated using the lower and upper bounds of the finite element limit analysis method. The effects of the setback distance ratio (L/B), excavation height ratio (H/B), soil strength heterogeneity (kB/c_u), and horizontal earthquake coefficient (k_h) were analyzed. Design charts and tables were produced to clarify the relationship between the undrained seismic bearing capacity and the selected parameters.

KEYWORDS excavation, finite element limit analysis, heterogeneous soil, strip footing, undrained bearing capacity

1 Introduction

Unsupported excavations in cohesive soils are typically utilized in different civil engineering structures, such as footings, piers, water and oil tanks, raft foundations, and retaining structures. They also comprise a part of the cut-and-cover method used for constructing shallow underground structures, such as underpasses and pipelines. Sufficient undrained shear strength of cohesive soil leads to the stability of unsupported excavations under short-term undrained conditions. This eliminates the need for constructing retaining walls to resist lateral earth pressure and reduces the construction cost and time of projects. Therefore, a precise stability analysis of such excavations is necessary [1–8].

A geotechnical engineer may encounter situations where a footing must be built near a vertical excavation. This typically occurs when the basement of a multistory building is constructed [9]. These conditions can influence the ultimate load that a footing can resist. Numerous researchers have investigated the bearing capacity of footings located on the flat ground [10–14]. In addition, some researchers have considered the influence of slopes and excavations on the stability and static and seismic bearing capacities of footings [15]. Kumar and Mohan Rao [16] examined how the pseudostatic horizontal earthquake coefficient influences the bearing capacity of footings near slopes, considering various ground inclinations. Azzouz and Baligh [17] assessed the impact of strip and square loads on the stability of slopes containing cohesive soil and provided design charts and tables for slope stability analysis. In terms of methods applied to estimate the bearing capacity, the stress characteristics method has been adopted for strip footings close to cohesionless slopes [18]. Shiau and Watson [19] considered a deep excavation site and assessed the bearing capacity of a footing. Georgiadis [20] employed the finite element analysis, upper bound plasticity, and stress field methods by concentrating the load inclination impact on the bearing capacity of strip footings sited close to the slopes. Georgiadis [21] used the finite element method to determine the undrained bearing capacity of footings close to slopes. The study suggested that three failure surfaces can be formed depending on the ratio of the slope height to the footing width. Shiau et al. [9] adopted the lower and upper bounds of the finite

Article history: Received May 12, 2022; Accepted Sep 7, 2022

element limit analysis (FELA) to evaluate the undrained bearing capacity of a strip footing near a slope. Experimental investigations on the bearing capacity of a strip footing close to a cohesionless slope have also shown that a direct relationship exists between the bearing capacity and the setback distance, defined as the distance between the footing and the slope crest [22,23]. In addition, the finite element lower bound approach was applied to assess the maximum load sustained by a strip footing on a slope [24]. Leshchinsky and Xie [25] computed the bearing capacities of strip footings sited near slopes consisting of cohesive-frictional soils by applying a limit analysis (LA) using discontinuity layout optimization (DLO). Halder et al. [26] assessed the bearing capacity of a strip footing close to a slope by adopting the lower bound of FELA. Zhou et al. [27] plotted design charts for strip footings resting on slopes using DLO. They reported that a direct nonlinear relationship exists between the normalized bearing capacity and the distance between the slope crest and footing.

The aim of this study was to compute the undrained seismic bearing capacity of a strip footing placed on an excavation consisting of heterogeneous soil. This study focused on isotropic soil analysis with deterministic heterogeneity without considering the superstructural inertial effect. The problem is first explained in the following section. Next, a comparison of the results of this study with those obtained by other researchers is presented. Design charts and tables are then provided. Finally, a design case is presented to clarify the solution procedure.

2 Problem definition

2.1 Model geometry

The geometric features of this study are depicted in Fig. 1. The undrained seismic bearing capacity of a strip footing located close to excavation is influenced by three parameters: geometrical features of the excavation, soil strength properties, and the horizontal earthquake coefficient. Thus, the undrained seismic bearing capacity of a strip footing can be written as Eq. (1):

$$\frac{q_u}{\gamma B} = f\left(\frac{L}{B}, \frac{H}{B}, k_h, \frac{c_u}{\gamma B}, \frac{kB}{c_u}\right), \tag{1}$$

where q_u is the average value obtained from the lower and upper bounds of FELA, B is the footing width (B = 1 m), H is the excavation height, L is the distance between the footing and the excavation, c_u is the undrained shear strength of the soil, k is the strength gradient with depth, γ is the unit weight of soil, and k_h is the horizontal earthquake coefficient.

In heterogeneous soil (Fig. 1), a direct relationship exists between the undrained shear strength and depth, as expressed by Eq. (2) [28–32].

$$c_u = c_{u0} + kz, \tag{2}$$

where c_{u0} is the undrained shear strength of soil at ground surface level.

2.2 Numerical analysis

The method of lower [33] and upper bounds [34], coupled

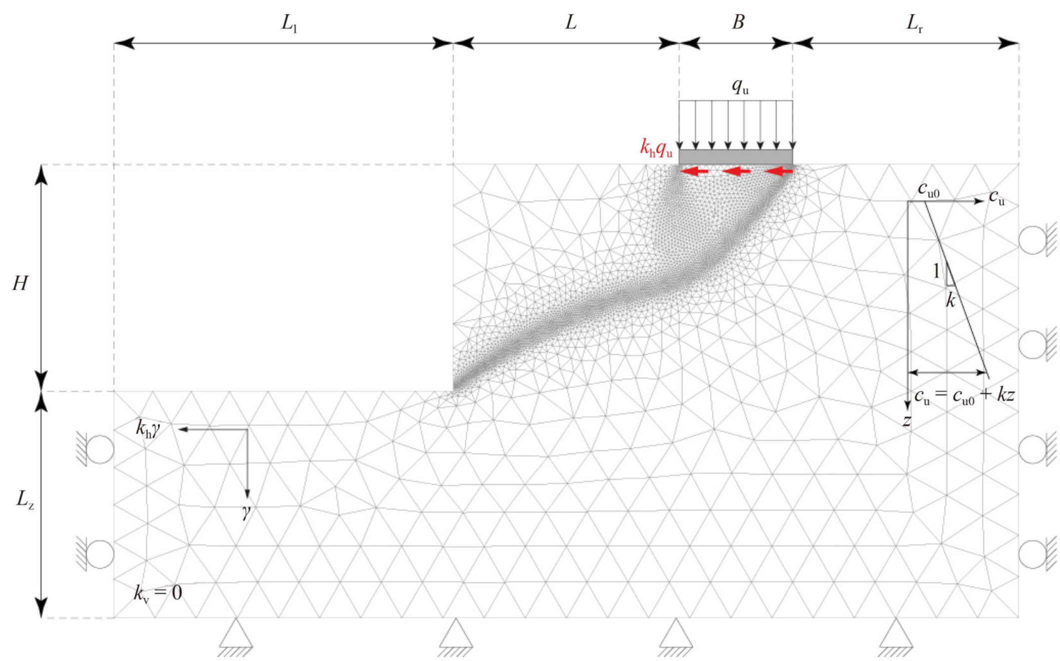

Fig. 1 Model geometry and typical FELA mesh. (Note: Dimensions are not on the main scale.)

with the finite element method, was used to calculate the undrained bearing capacity of a strip footing considering all influential parameters, as expressed by Eq. (1). The formulation of these methods and the general computational procedure were proposed by Sloan [33,34]. These methods have been well-described in Refs. [13,35].

OptumG2 [36], which uses FELA and a linear programming approach, was used to determine the undrained seismic bearing capacity of a strip footing adjoining an excavation. A sensitivity analysis was conducted to determine the initial number of elements, ultimate number of elements, and final dimensions of the model to ensure that the results were not influenced by the boundaries [37–39]. Consequently, the initial number of elements was set to 5000, and the ultimate number of elements reached 10000 in three iterations. In the most critical cases, L_r, L_l, and L_z are equal to 9B, 10B, and 5B, respectively (L_r, L_l, and L_z are illustrated in Fig. 1). The associated Mohr−Coulomb failure criterion was assigned to the soil, and the footing was modeled by adopting a weightless plate element [29,37,40]. The interface between the footing and soil was modeled as perfectly rough (δ/φ = 1) and perfectly smooth (δ/φ = 0) [41–43]. The bottom of the model was constrained in vertical and horizontal directions. In contrast, the two sides could move vertically (Fig. 1). The pseudostatic approach was utilized in the model to simulate horizontal earthquakes [42,44].

3 Comparison with results of previous studies

A comparison was made with the results of other studies to verify the results of this study. Shiau et al. [9] adopted finite-element lower and upper bounds and calculated the bearing capacity of strip footings on a homogenous soil excavation under undrained conditions (β = 90°). Chen and Xiao [45] proposed a solution for the undrained bearing capacity of strip footings near a slope using the upper bound of FELA. Table 1 presents comparisons between the results of the upper bound analysis of this study and those of Shiau et al. [9] and Chen and Xiao [45]. Slight differences between the results of this study and those of the other two studies were observed.

Gourvenec and Mana [30] applied the FEM to calculate the bearing capacity factors of strip footings and incorporated strength heterogeneity in their solutions. In addition, as listed in Table 2, the values of N_c for different kB/c_u ratios obtained in this study and those of Gourvenec and Mana [30] are consistent. The values obtained in their study are within the values obtained from the lower and upper bounds solutions of FELA.

Moreover, values of $q_u/(\gamma B)$ were computed using the lower and upper bounds for a smooth strip footing resting on the level ground under undrained conditions. The results were compared with those of Shiau et al. [9], Mofidi Rouchi et al. [24], and Foroutan Kalourazi et al. [46], in which the same method used in this study was adopted. The comparisons in Table 3 show that the results are in good agreement.

Finally, the bearing capacity factor (N_γ) values calculated for the strip footing on level ground in this study and other studies using methods including LB, UB, stress characteristic (SC), and limit equilibrium (LE) are presented in Table 4. Table 4 shows that their results are consistent.

Table 1 Validation of $q_u/(\gamma B)$ (upper bound values) for homogenous soil excavation (β = 90°)

L/B	$c_u/(\gamma B)$	Shiau et al. [9]	Chen and Xiao [45]	present study
0	1	1.32 (1.32)	1.41	1.13 (1.13)
	3	5.50 (5.50)	5.48	5.58 (5.62)
	5	9.50 (9.50)	9.49	9.66 (9.74)
	10	19.95 (19.95)	19.50	19.68 (20.03)
1	1	1.20 (1.20)	1.29	1.07 (1.07)
	3	9.01 (9.01)	8.86	8.84 (8.89)
	5	16.12 (16.17)	15.90	15.88 (15.90)
	10	33.75 (33.79)	33.29	33.18 (33.30)
2	1	1.46 (1.46)	1.37	1.27 (1.27)
	3	10.85 (10.88)	10.87	10.71 (10.72)
	5	19.64 (19.65)	20.10	19.45 (19.47)
	10	41.31 (41.33)	42.68	40.90 (40.98)
3	1	1.99 (1.99)	1.93	1.91 (1.92)
	3	12.72 (12.78)	12.98	12.57 (12.62)
	5	22.73 (22.74)	23.67	22.44 (22.49)
	10	47.30 (47.32)	50.27	46.76 (46.84)

Note: Values outside and within parentheses correspond to smooth and rough footings, respectively.

Table 2 Validation of bearing capacity factor, N_c, for strip footing on level ground

kB/c_u	Gourvenec and Mana [30]	present study	
		LB[a]	UB[b]
0	5.144 (5.175)[c]	5.027 (5.069)	5.196 (5.233)
5	8.357 (9.818)	7.733 (9.521)	8.519 (9.977)
20	14.702 (17.457)	13.433 (16.708)	15.065 (17.779)
100	40.594 (46.456)	34.460 (43.439)	41.776 (47.581)
200	69.563 (77.805)	60.080 (71.388)	72.196 (79.815)

Notes: a) LB: lower bound; b) UB: upper bound; c) values outside and within parentheses correspond to smooth and rough footings, respectively.

4 Results and discussion

4.1 Seismic threshold value

The seismic threshold value is the value of k_h above which the strip footing slides (Fig. 2(a)). The variations in $k_h \times q_u/c_u$ versus k_h for a strip footing near an excavation are shown in Fig. 2. The threshold value decreased as kB/c_u increased (Fig. 2). For instance, the threshold value was 0.78 when $kB/c_u = 0$ (homogenous soil), whereas it reached 0.14 for soil with $kB/c_u = 20$ (Fig. 2). Moreover, as the L/B ratio increased, the threshold value decreased to a constant value for higher ratios, and the ratio at which this value became constant increased as kB/c_u decreased. The threshold values for soils with $kB/c_u = 20$ and 10 remained unchanged for L/B values exceeding 0.25, and for those with $kB/c_u = 2$ and 5, they stabilized at $L/B = 0.5$. However, for soils with $kB/c_u = 1$ and 0, the threshold value did not change when L/B exceeded 1 and 2, respectively. Regarding the influence of H/B, when $kB/c_u = 2$, 5, 10, or 20, the value of $k_h \times q_u/c_u$ was not influenced by H/B. However, when $kB/c_u = 0$ and 1, H/B could affect the soil. At $kB/c_u = 0$, H/B could not influence the soil when $L/B \geqslant 3$. At $kB/c_u = 1$, the effect of H/B on the soil became minimal when $L/B \geqslant 2$.

4.2 Design charts

Design charts and tables were developed for a strip footing adjoining an excavation of homogenous or heterogeneous soils. The variation in $q_u/(\gamma B)$ for $k_h = 0$, the effect of L/B and H/B on the failure pattern, and finally the variation in $q_u/(\gamma B)$ for $k_h \neq 0$, are depicted in Figs. 3 and 4, Figs. 5 and 6, and Figs. 7–10, respectively.

Under $k_h = 0$ conditions, the rough footing had slightly higher $q_u/(\gamma B)$ values than the smooth (frictionless) footing for a specific value of $c_u/(\gamma B)$, as expected (Figs. 3 and 4). For the rough and smooth footings, the most significant trend in Figs. 3 and 4 is the direct relationship between kB/c_u and $q_u/(\gamma B)$. As $c_u/(\gamma B)$ increased from 0.5 to 5, $q_u/(\gamma B)$ increased for all values of kB/c_u, reaching approximately 10 times as high as its initial value at $c_u/(\gamma B) = 0.5$. For a fixed value of $c_u/(\gamma B)$, $q_u/(\gamma B)$ converged to its maximum value at a lower L/B when kB/c_u increased. That is, for a smooth footing on soil with $c_u/(\gamma B) = 0.5$ and $kB/c_u = 5$ (Fig. 3), $q_u/(\gamma B)$ reached its peak value at an L/B value of approximately 0.8, whereas this ratio was approximately 0.3 for soil with $kB/c_u = 20$. The variation in the ultimate bearing capacity of the rough footing with the L/B ratio is depicted in Fig. 5 for soil with $H/B = 2$, $c_u/(\gamma B) = 1$, $kB/c_u = 0.5$, and $k_h = 0.25$.

Furthermore, H/B can impact $q_u/(\gamma B)$ in soils with low kB/c_u values, regardless of whether the footing is rough or smooth (Figs. 3 and 4). When $kB/c_u = 5$, 10, and 20, only one curve appeared, indicating that for a fixed L/B ratio, $q_u/(\gamma B)$ did not change as H/B varied. In contrast, the H/B ratio influenced $q_u/(\gamma B)$ in soils with $kB/c_u = 0$, 1, and 2. The impact of variations in H/B was more significant in homogenous soils than in heterogeneous soils. Figure 6 shows the effect of H/B on $q_u/(\gamma B)$ for a rough footing with $L/B = 1.5$ on soil with $c_u/(\gamma B) = 3$, $kB/c_u = 0.5$, and $k_h = 0.05$. At $c_u/(\gamma B) = 0$, the footing can only be constructed near excavations with $H/B = 0.5$ or 1. However, as $c_u/(\gamma B)$ increases, the footing can be sited adjacent to excavations with higher H/B values, that is, $H/B = 10$, although the $q_u/(\gamma B)$ values are the lowest for such H/B.

Table 3 Validation of $q_u/(\gamma B)$ under undrained conditions for the range of $c_u/(\gamma B)$ of perfectly smooth footing ($L/B = 1$) on level ground

$c_u/(\gamma B)$	Shiau et al. [9][a)]	Mofidi Rouchi et al. [24][b)]	Foroutan Kalourazi et al. [46][c)]	present study	
				LB	UB
2	5.02	4.10	4.28	4.43	4.82
4	12.36	11.02	11.38	11.68	12.14
6	19.46	17.99	18.36	18.52	19.06
8	26.13	24.54	25.09	25.74	26.12
10	32.93	30.91	31.82	31.96	32.68

Notes: a) Average values for finite element lower and upper bounds LA; b) values for finite element lower bound LA; c) values for finite element lower bound LA (number of inscribed polygon vertices (np) = 24).

Table 4 Validation of bearing capacity factor, N_γ, for perfectly smooth and rough footings [35]

soil-foundation interface	φ (°)	Ukritchon et al. [47]		Hjiaj et al. [48]		Kumar and Kouzer [49]	Kumar [50]	Kumar and Chakraborty [51]	Veiskarami et al. [13]	Pakdel et al. [52]	Izadi et al. [42]	present study	
		LB[a)]	UB[a)]	LB[b)]	UB[b)]	UB	SC	LB	LB	LE	LB	LB	UB
perfectly smooth ($\delta = 0$)	10	0.27	0.30	0.28	0.30	0.31	0.28	0.29	0.29	0.33	0.29	0.27	0.29
	20	1.52	1.73	1.58	1.67	1.74	1.57	1.59	1.59	1.62	1.59	1.54	1.71
	30	7.18	8.54	7.62	8.08	8.47	7.65	7.58	7.85	7.9	7.85	7.56	8.28
	40	38.5	54.2	42.77	45.42	50.38	43.08	41.95	43.9	44.25	41.59	40.17	49.53
perfectly rough ($\delta = \varphi$)	10	0.41	0.47	0.43	0.46	0.49	0.43	0.43	0.44	0.47	0.44	0.42	0.48
	20	2.67	3.27	2.82	2.96	3.16	2.82	2.82	2.88	3.12	2.89	2.75	3.18
	30	13.2	17.4	14.57	15.24	16.64	14.68	14.53	15.03	15.25	15.06	13.72	16.92
	40	69.9	111.1	83.33	88.39	98.53	85.01	81.8	70.62	77.75	79.19	75.96	97.83

Notes: a) Lower and upper bounds limit analyses combined with finite elements and linear programming; b) lower and upper bounds limit analyses combined with nonlinear programming.

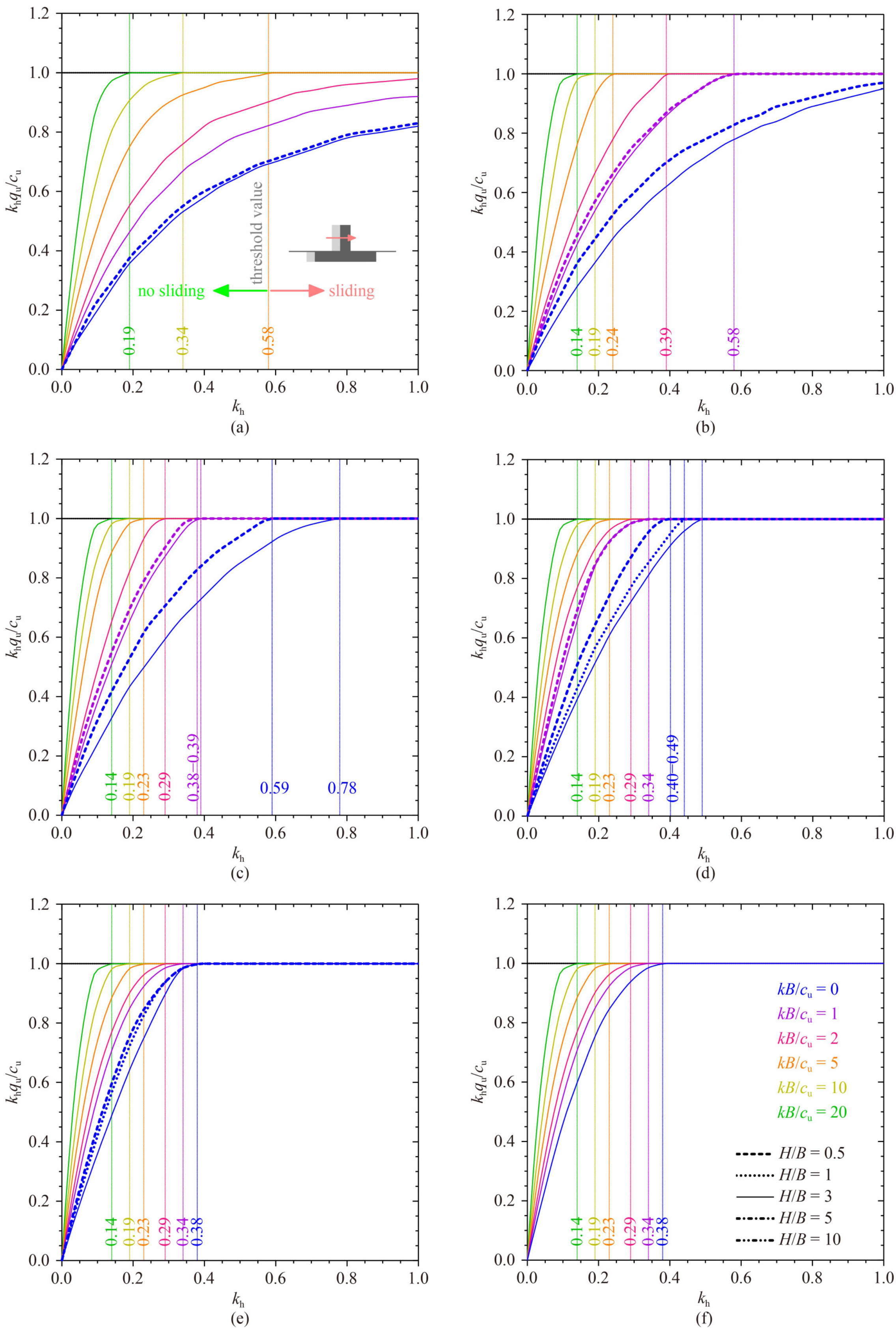

Fig. 2 Graphs for $q_u k_h/c_u$ versus k_h for various conditions of L/B and H/B. (a) $L/B = 0$; (b) $L/B = 0.25$; (c) $L/B = 0.5$; (d) $L/B = 1$; (e) $L/B = 2$; (f) $L/B \geqslant 3$.

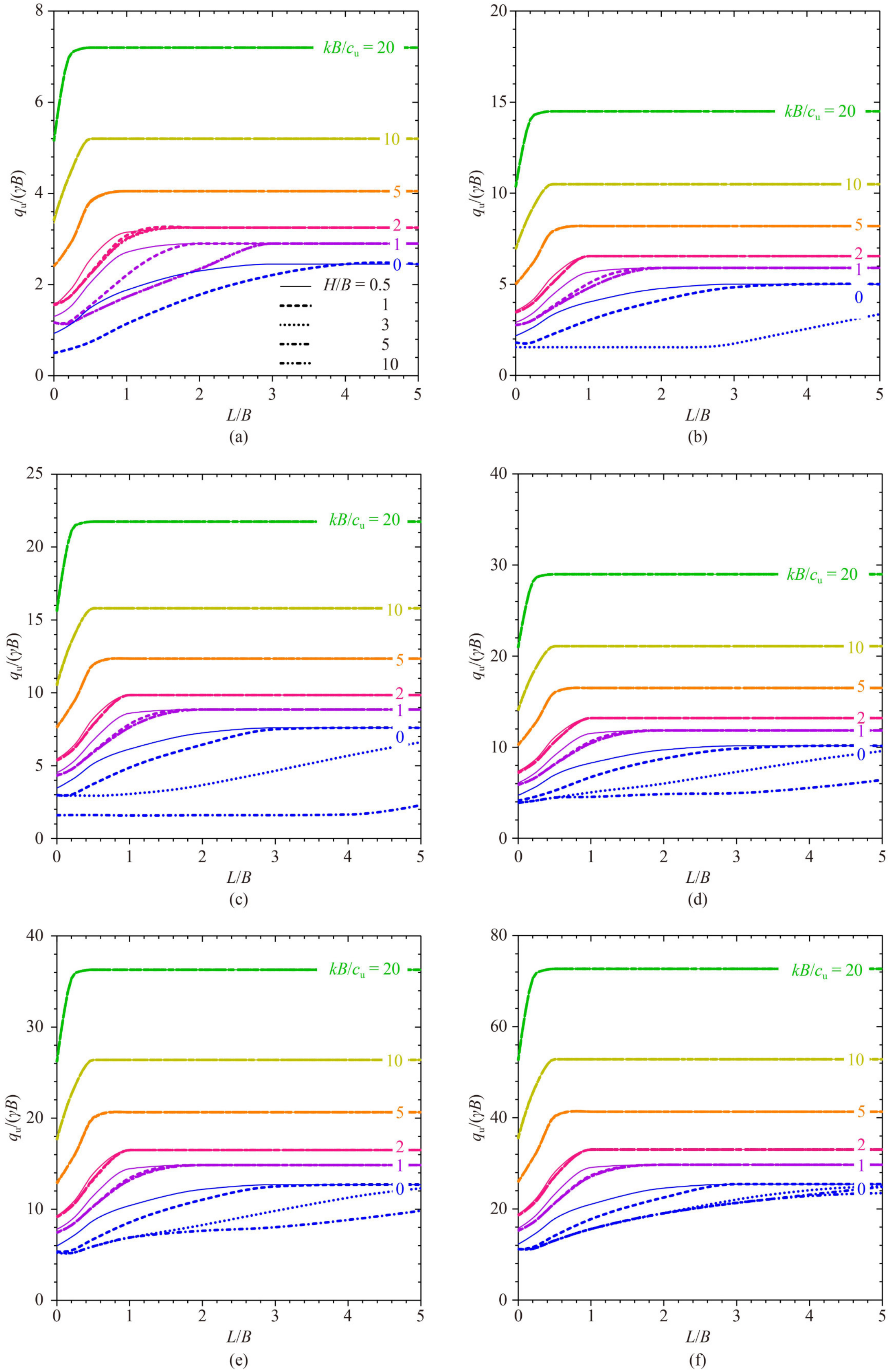

Fig. 3 Mean values of $q_u/(\gamma B)$ for smooth strip footing adjoining excavation ($k_h = 0.0$). (a) $c_u/(\gamma B) = 0.5$; (b) $c_u/(\gamma B) = 1.0$; (c) $c_u/(\gamma B) = 1.5$; (d) $c_u/(\gamma B) = 2.0$; (e) $c_u/(\gamma B) = 2.5$; (f) $c_u/(\gamma B) = 5.0$.

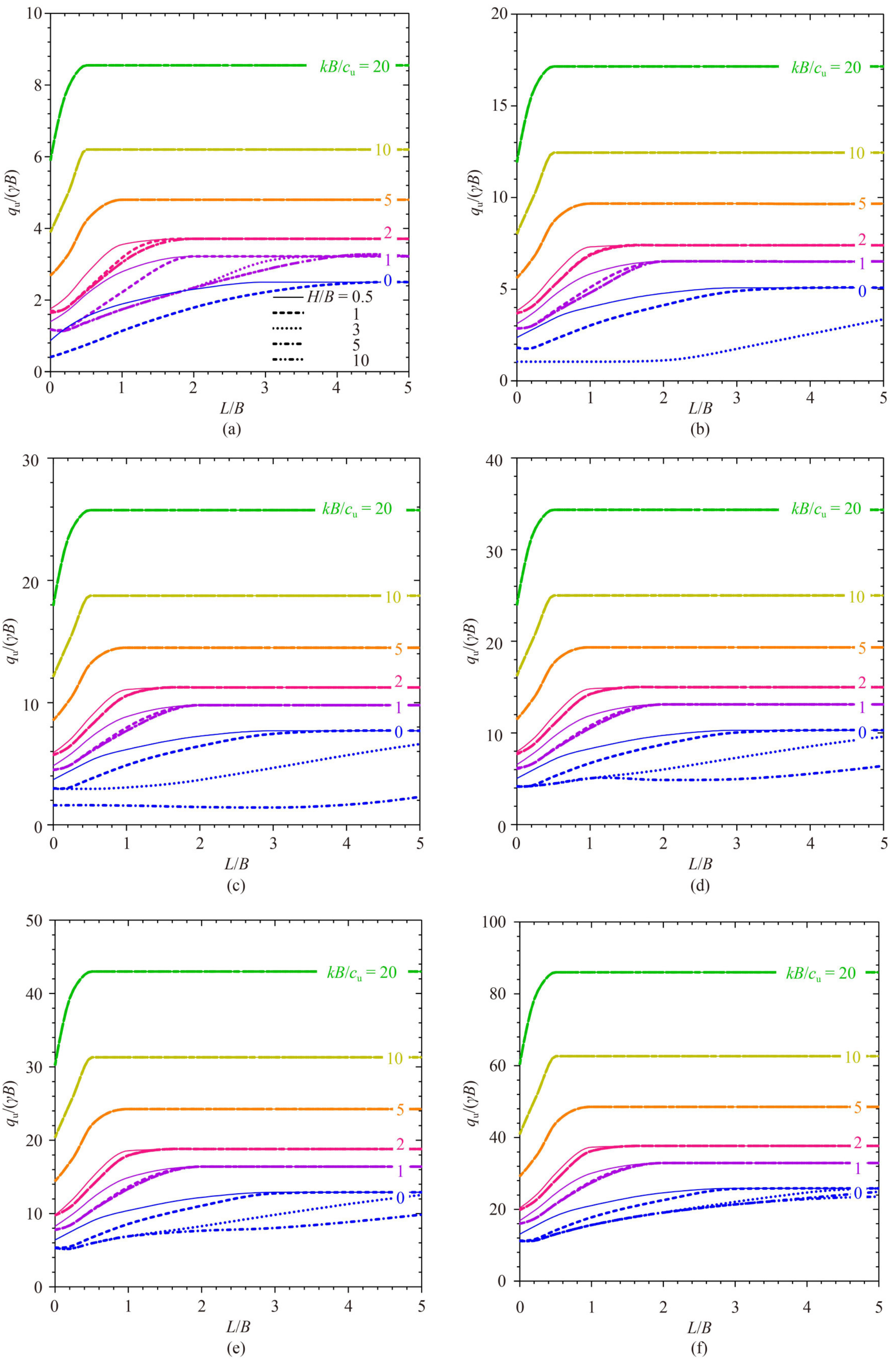

Fig. 4 Mean values of $q_u/(\gamma B)$ for rough strip footing adjoining excavation ($k_h = 0.0$). (a) $c_u/(\gamma B) = 0.5$; (b) $c_u/(\gamma B) = 1.0$; (c) $c_u/(\gamma B) = 1.5$; (d) $c_u/(\gamma B) = 2.0$; (e) $c_u/(\gamma B) = 2.5$; (f) $c_u/(\gamma B) = 5.0$.

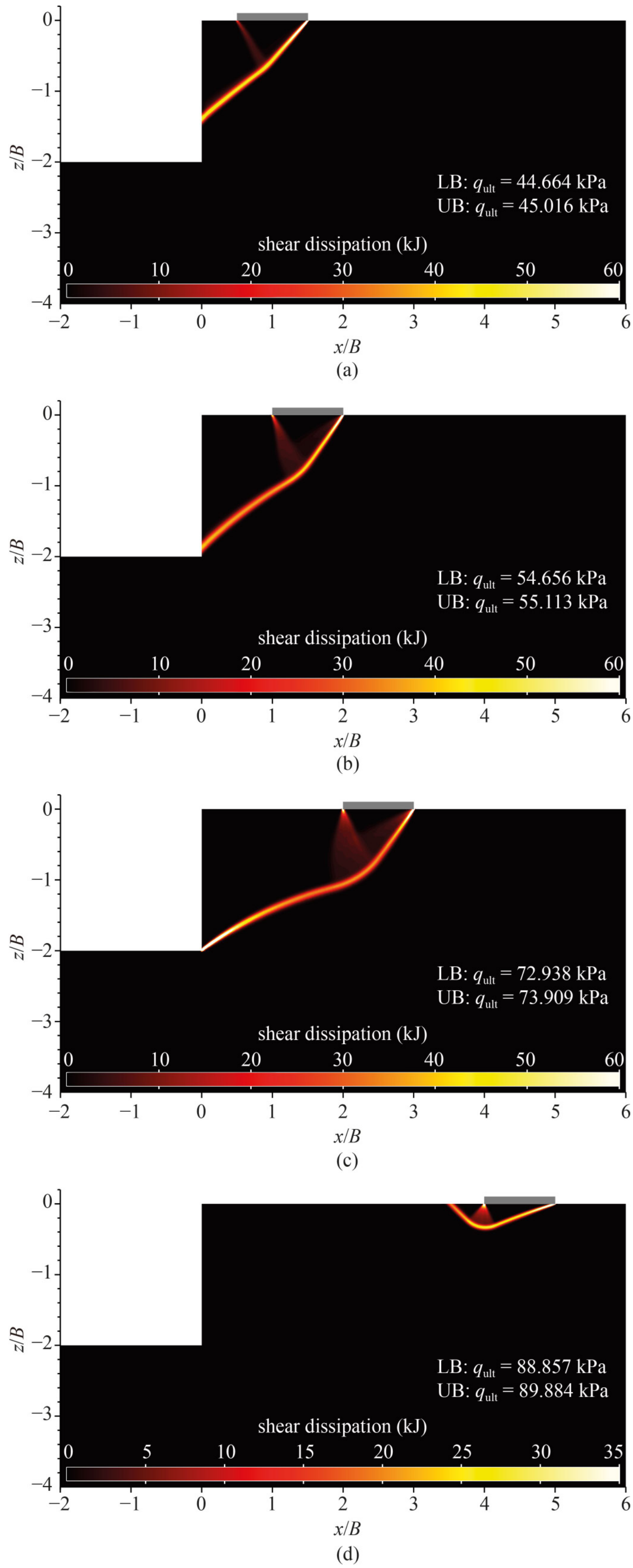

Fig. 5 Effect of L/B on ultimate bearing capacity ($H/B = 2$, $c_u/(\gamma B) = 1$, $kB/c_u = 0.5$, $k_h = 0.25$, rough footing). (a) $L/B = 0.5$; (b) $L/B = 1$; (c) $L/B = 2$; (d) $L/B = 4$.

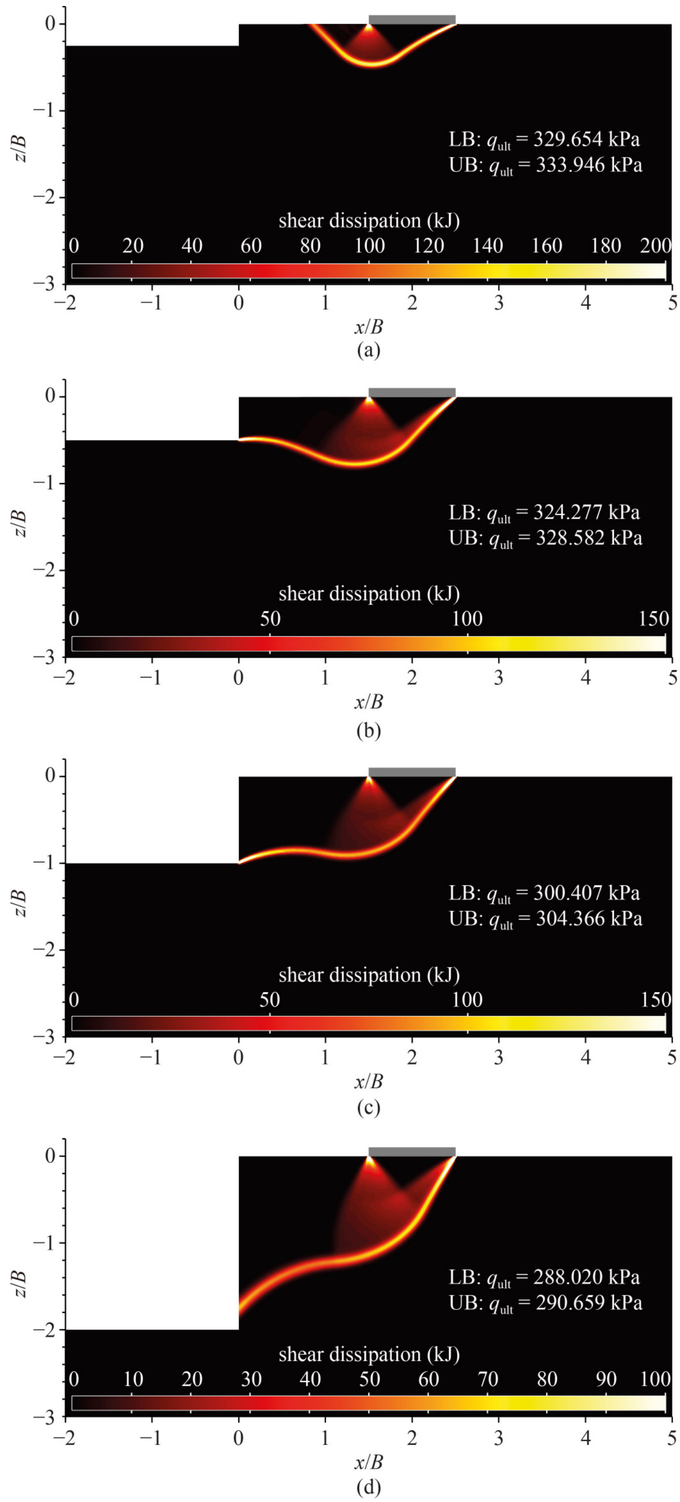

Fig. 6 Effect of H/B on ultimate bearing capacity ($c_u/(\gamma B)$ = 3, kB/c_u = 0.5, k_h = 0.05, rough footing). (a) L/B = 0.25; (b) L/B = 0.5; (c) L/B = 1; (d) L/B = 2.

However, when $k_h \neq 0$, H/B and $c_u/(\gamma B)$ impact $q_u/(\gamma B)$, similar to the $k_h = 0$ conditions. At a specific k_h and kB/c_u, $q_u/(\gamma B)$ increased 10-fold when $c_u/(\gamma B)$ increased from 0.5 to 5 (Figs. 7–10). In addition, the H/B ratio can influence soils with kB/c_u = 0, 1, and 2 (Figs. 7–10). However, when $k_h > 0.2$ and $c_u/(\gamma B)$ = 0.5 and 1, a strip footing cannot be constructed on homogenous soil owing to stability problems (kB/c_u = 0) (Figs. 9 and 10). Similarly, at k_h = 0.2 and $c_u/(\gamma B)$ = 0.5, the excavation in homogenous soils becomes unstable (Fig. 8).

Moreover, the effect of L/B on $q_u/(\gamma B)$ decreased with an increase in k_h. In soils with kB/c_u = 20 and 10, $q_u/(\gamma B)$

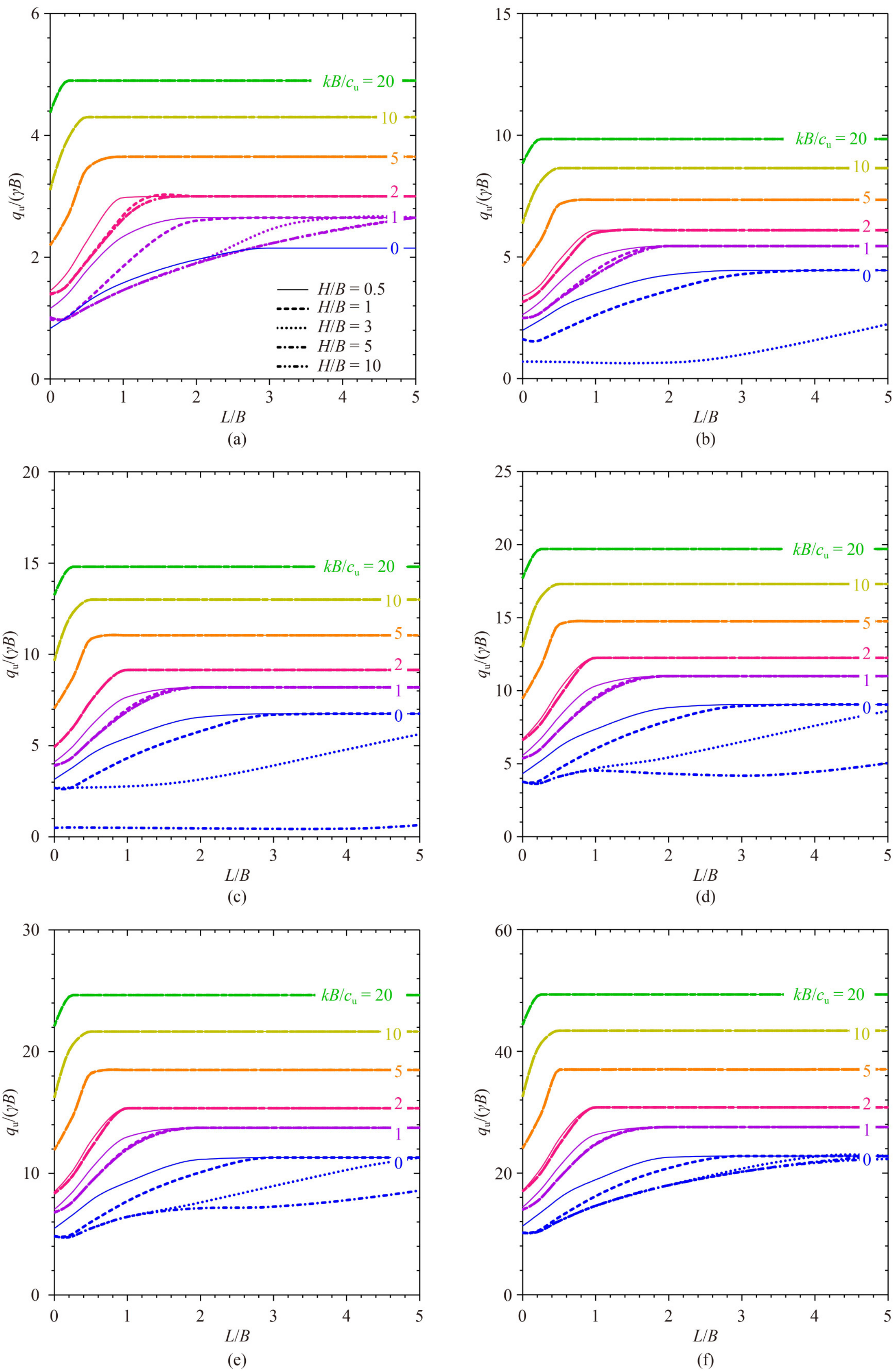

Fig. 7 Mean values of $q_u/(\gamma B)$ for rough strip footing adjoining excavation ($k_h = 0.1$). (a) $c_u/(\gamma B) = 0.5$; (b) $c_u/(\gamma B) = 1.0$; (c) $c_u/(\gamma B) = 1.5$; (d) $c_u/(\gamma B) = 2.0$; (e) $c_u/(\gamma B) = 2.5$; (f) $c_u/(\gamma B) = 5.0$.

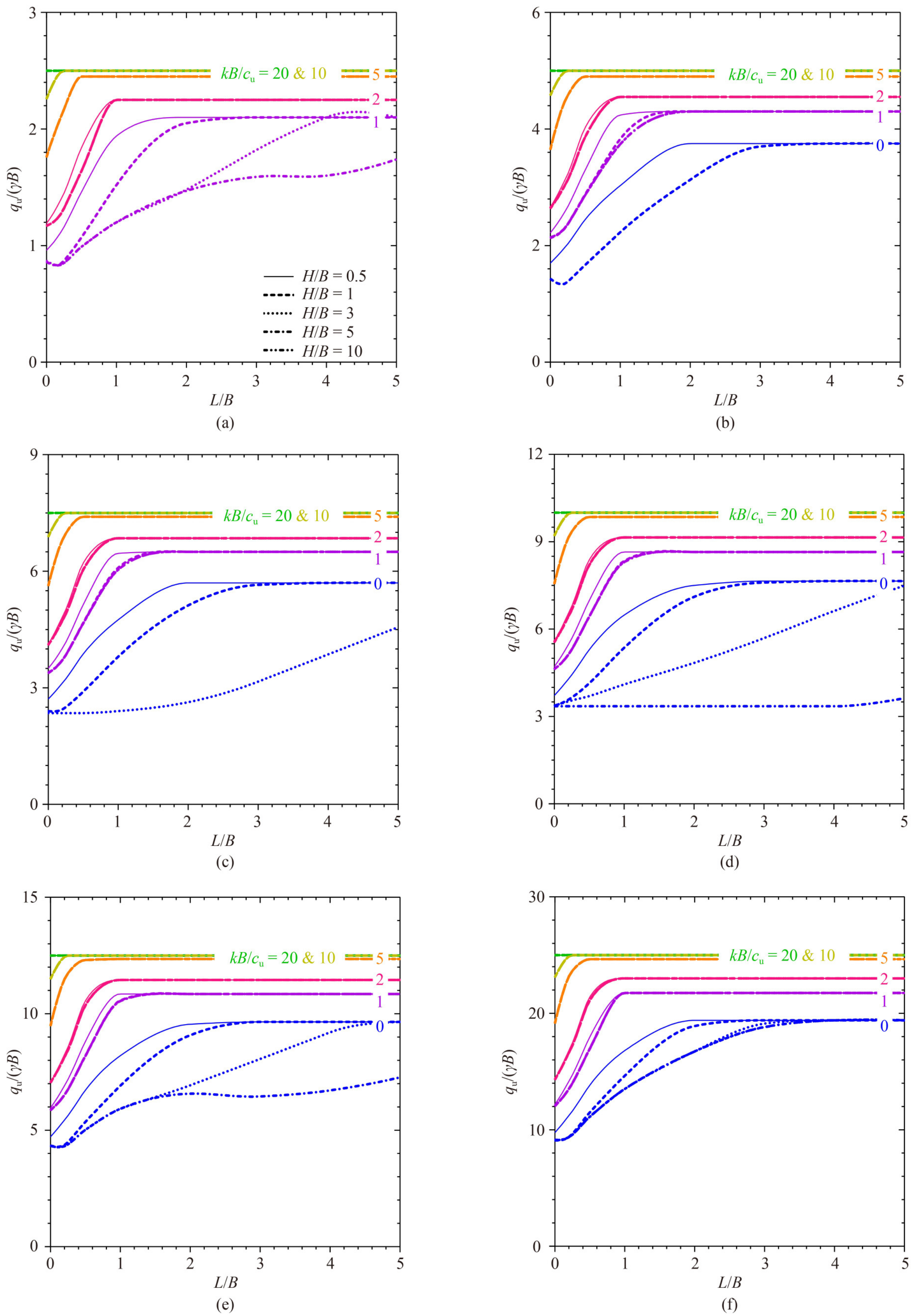

Fig. 8 Mean values of $q_u/(\gamma B)$ for rough strip footing adjoining excavation (k_h = 0.2). (a) $c_u/(\gamma B)$ = 0.5; (b) $c_u/(\gamma B)$ = 1.0; (c) $c_u/(\gamma B)$ = 1.5; (d) $c_u/(\gamma B)$ = 2.0; (e) $c_u/(\gamma B)$ = 2.5; (f) $c_u/(\gamma B)$ = 5.0.

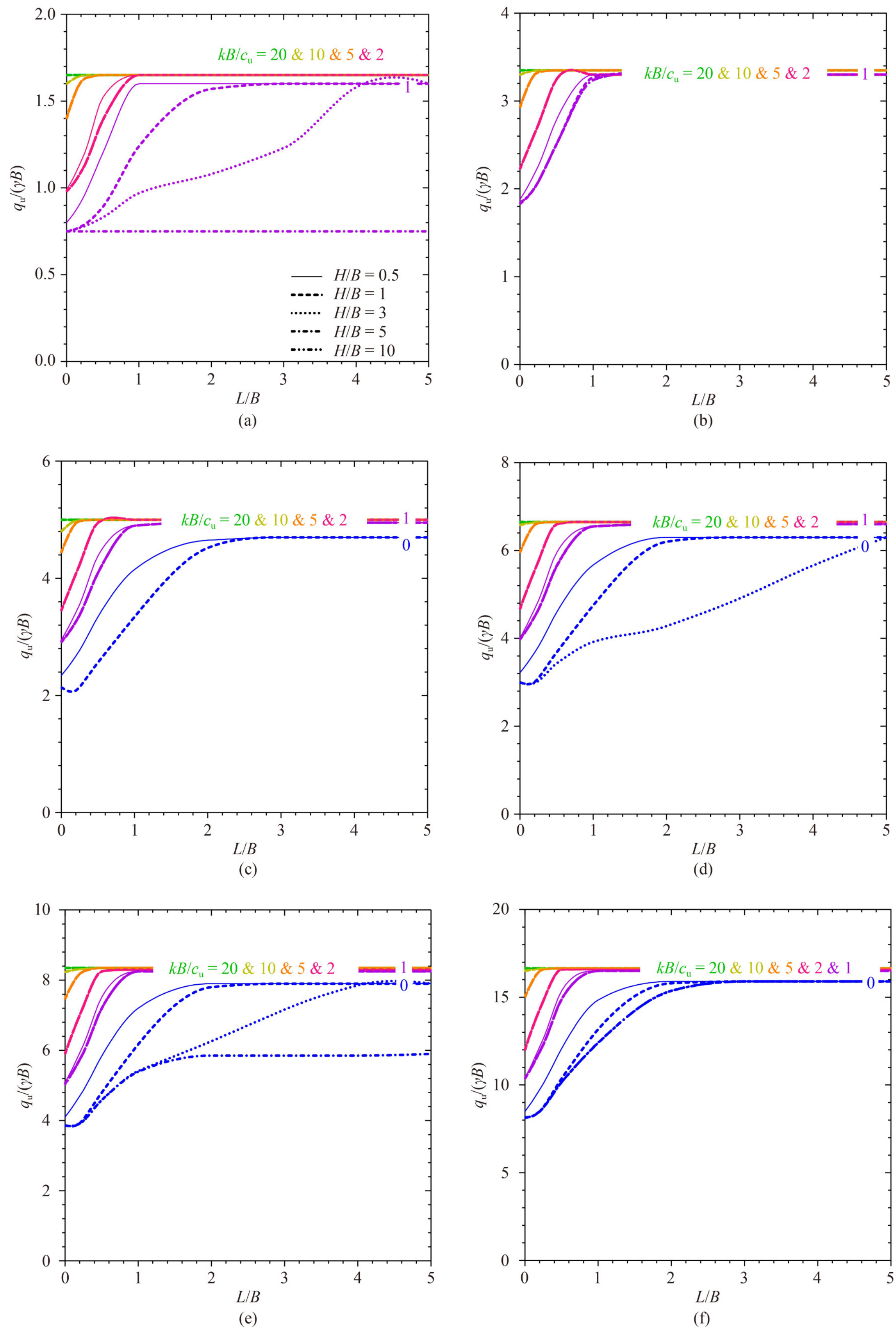

Fig. 9 Mean values of $q_u/(\gamma B)$ for rough strip footing adjoining excavation (k_h = 0.3). (a) $c_u/(\gamma B)$ = 0.5; (b) $c_u/(\gamma B)$ = 1.0; (c) $c_u/(\gamma B)$ = 1.5; (d) $c_u/(\gamma B)$ = 2.0; (e) $c_u/(\gamma B)$ = 2.5; (f) $c_u/(\gamma B)$ = 5.0.

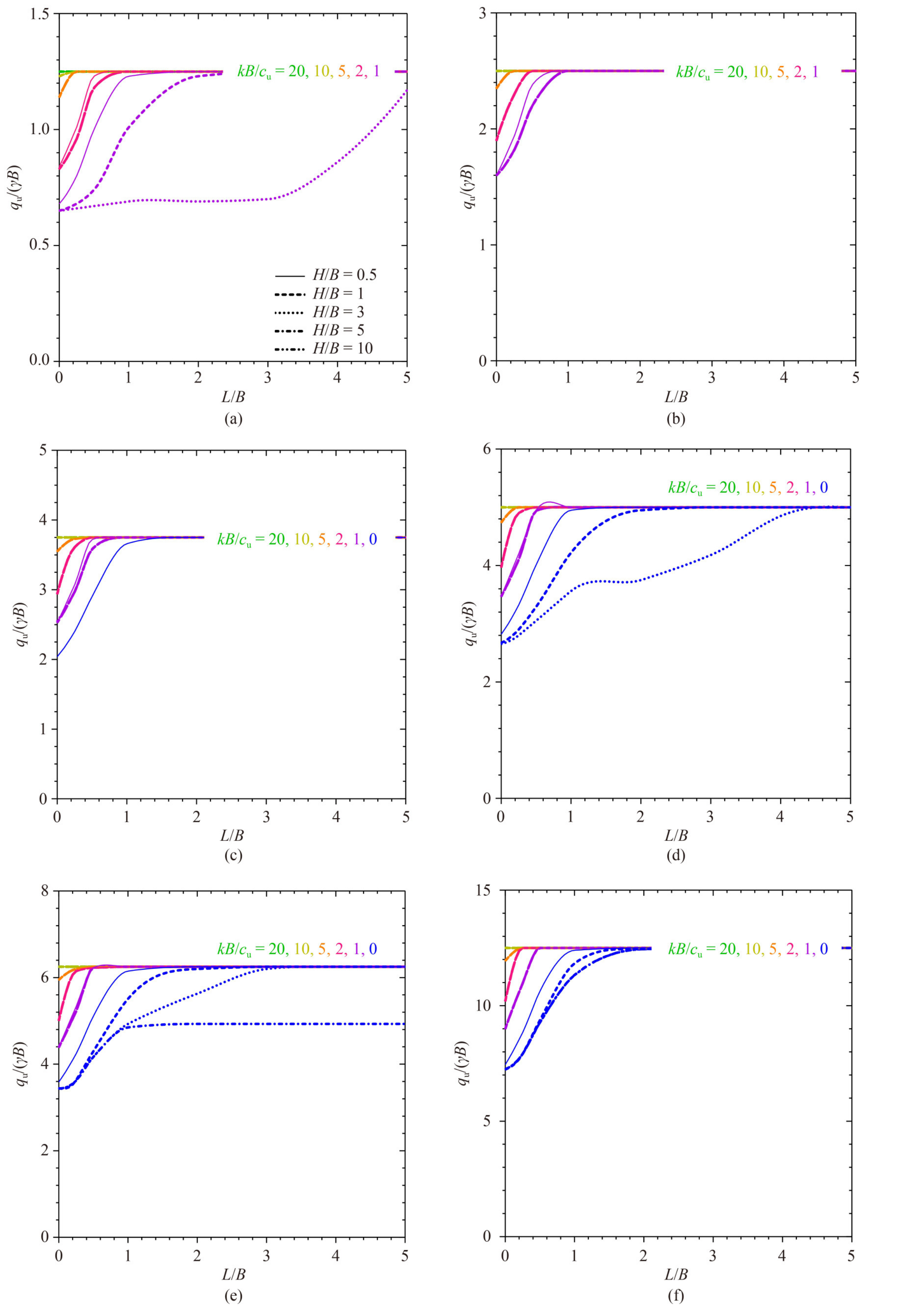

Fig. 10 Mean values of $q_u/(\gamma B)$ for rough strip footing adjoining excavation ($k_h = 0.4$). (a) $c_u/(\gamma B) = 0.5$; (b) $c_u/(\gamma B) = 1.0$; (c) $c_u/(\gamma B) = 1.5$; (d) $c_u/(\gamma B) = 2.0$; (e) $c_u/(\gamma B) = 2.5$; (f) $c_u/(\gamma B) = 5.0$.

attained its highest value over the range of L/B when $k_h > 0.1$ and $k_h > 0.2$, respectively (Figs. 8–10). This implies that in such soils, $q_u/(\gamma B)$ is not influenced by L/B. Similarly, for soils with kB/c_u = 0, 1, 2, and 5, the value of L/B at which $q_u/(\gamma B)$ converged to its maximum value decreased as k_h increased, with the lowest values at k_h = 0.4.

The increase in k_h resulted in a decreased $q_u/(\gamma B)$ (Figs. 7–10); that is, for the soil with $c_u/(\gamma B)$ = 0.5 and kB/c_u = 20, the maximum value of $q_u/(\gamma B)$ was almost 5 at k_h = 0.1 (Fig. 7), whereas it decreased to more than 1.2 at k_h = 0.4 (Fig. 10). In addition, as k_h increased, the differences between the values of $q_u/(\gamma B)$ for soils with different kB/c_u values decreased such that the values converged for all cases of kB/c_u and $c_u/(\gamma B)$ when k_h increased to 0.4.

Values of q_u for different H/B, $c_u/(\gamma B)$, and kB/c_u values were obtained for the most critical conditions of L/B (i.e., L/B = 0) and various k_h (Tables 5 and 6) for perfectly smooth and perfectly rough footings. As the perfectly smooth footing slides when subjected to seismic loads owing to the lack of friction, this footing was only analyzed statically (k_h = 0). The *NaN* in the tables denoting "not a number" indicates that q_u was not calculated because of the instability of the excavation.

Table 5 Values of q_u (kPa) at L/B = 0 for footing adjoining excavation (kB/c_u = 0 and 1)

$c_u/(\gamma B)$	H/B	kB/c_u = 0					kB/c_u = 1				
		k_h = 0.0	k_h = 0.1	k_h = 0.2	k_h = 0.3	k_h = 0.4	k_h = 0.0	k_h = 0.1	k_h = 0.2	k_h = 0.3	k_h = 0.4
0.5	0.5	(18.68) 17.39	16.59	–	–	–	(25.92) 27.97	23.15	19.21	16.03	13.53
	1	(10.11) 8.11	–	–	–	–	(23.41) 23.65	19.69	17.29	14.69	12.53
	3	–	–	–	–	–	(23.40) 23.65	20.28	17.30	14.70	12.54
	5	–	–	–	–	–	(23.45) 23.65	20.27	17.24	14.67	*NaN*
	10	–	–	–	–	–	(23.41) 23.51	20.26	*NaN*	*NaN*	*NaN*
1	0.5	(43.67) 47.31	39.88	33.94	–	–	(58.20) 62.41	52.68	44.30	37.52	32.26
	1	(36.05) 36.19	32.35	28.67	–	–	(55.24) 57.11	49.79	42.64	36.64	32.64
	3	(30.94) 31.06	25.82	–	–	–	(55.42) 57.35	50.71	42.78	36.81	31.83
	5	–	–	–	–	–	(55.16) 57.10	49.67	42.78	36.80	31.89
	10	–	–	–	–	–	(55.17) 57.15	49.77	42.82	36.82	31.90
1.5	0.5	(69.13) 73.95	63.12	54.15	46.82	40.81	(90.32) 96.76	82.11	69.07	58.93	50.65
	1	(59.71) 59.95	53.88	48.06	42.76	–	(86.58) 90.18	78.66	67.61	58.15	50.54
	3	(59.01) 59.00	53.63	46.95	–	–	(86.22) 90.39	78.37	67.69	58.37	51.23
	5	(50.02) 50.40	6.43	–	–	–	(86.72) 89.78	78.68	67.74	58.36	50.57
	10	–	–	–	–	–	(86.94) 90.09	78.85	67.53	58.34	50.56
2	0.5	(94.35) 100.92	86.44	74.34	64.42	56.35	(121.54) 131.24	111.30	94.24	80.17	69.32
	1	(83.27) 83.59	75.24	67.42	60.08	53.33	(117.67) 123.47	107.32	92.54	79.53	69.07
	3	(82.89) 82.93	75.25	67.48	60.03	48.93	(118.07) 123.38	107.51	92.34	79.72	69.17
	5	(82.85) 82.99	75.34	67.46	–	–	(117.73) 123.12	107.38	92.59	79.78	69.11
	10	–	–	–	–	–	(118.21) 122.09	107.37	92.57	79.67	68.54
2.5	0.5	(119.52) 127.84	109.52	94.45	82.07	71.86	(157.01) 165.49	140.75	119.21	101.61	87.80
	1	(106.91) 107.04	96.88	86.76	77.22	68.71	(148.59) 155.77	135.70	117.40	101.02	87.42
	3	(104.13) 106.07	96.68	86.61	77.21	68.83	(149.61) 156.23	136.74	117.36	100.59	87.56
	5	(106.50) 106.36	96.85	86.68	77.22	68.87	(148.99) 156.19	136.13	117.16	101.10	87.43
	10	–	–	–	–	–	(148.82) 155.73	135.95	117.21	101.02	87.56
5	0.5	(245.45) 261.89	225.88	195.08	169.82	149.08	(314.90) 337.17	287.96	243.58	207.87	180.09
	1	(223.63) 225.69	204.20	181.79	163.53	144.84	(306.26) 320.98	279.90	241.12	207.32	179.26
	3	(224.59) 224.71	203.69	182.32	162.51	144.93	(305.77) 320.86	279.10	241.05	207.57	179.07
	5	(224.42) 224.15	204.01	182.55	162.59	144.96	(304.71) 321.03	280.15	241.27	207.61	179.91
	10	(223.82) 224.87	203.40	182.77	162.55	144.99	(305.66) 320.61	280.00	240.76	207.71	179.66

Note: The values inside and outside the brackets correspond to values for smooth and rough footings, respectively.

Table 6 Mean and standard deviation values of q_u (kPa) at $L/B = 0$ for strip footing adjoining excavation in full ranges of H/B ($kB/c_u = 2$, 5, 10, and 20)

soil-foundation interface	k_h	$c_u/(\gamma B)$	kB/c_u							
			2		5		10		20	
			mean	*SD*	mean	*SD*	mean	*SD*	mean	*SD*
perfectly smooth ($\delta = 0$)	0	0.5	30.815	0.786	48.053	0.106	67.964	0.696	102.523	0.262
		1	69.612	0.770	100.595	0.284	139.357	0.832	207.688	0.493
		1.5	107.844	0.818	152.684	0.900	211.327	0.789	312.741	1.199
		2	145.546	1.262	205.260	0.480	281.812	0.766	417.853	3.601
		2.5	183.780	1.018	256.138	3.828	351.594	4.670	520.176	5.783
		5	373.843	2.012	519.978	1.179	711.589	2.853	1049.911	3.931
perfectly rough ($\delta = \varphi$)	0	0.5	33.670	0.963	53.424	0.221	78.258	0.195	118.253	0.182
		1	74.420	1.245	112.295	0.127	160.953	0.413	239.816	0.822
		1.5	115.307	1.595	170.893	0.563	243.082	0.336	361.418	1.629
		2	155.714	2.151	229.932	0.270	325.793	0.714	481.924	1.824
		2.5	195.892	0.279	288.513	0.523	407.711	0.441	603.755	1.865
		5	400.044	4.257	583.593	1.238	819.858	1.008	1209.966	3.708
	0.1	0.5	28.150	0.523	44.114	0.296	62.366	0.357	87.737	0.282
		1	64.305	2.403	92.831	0.055	126.802	3.630	176.942	0.636
		1.5	97.916	0.580	141.305	0.166	194.301	0.563	265.494	0.043
		2	133.031	0.608	190.020	0.327	261.087	1.682	355.263	1.215
		2.5	168.077	1.533	239.038	0.061	325.944	0.855	443.232	0.504
		5	340.585	1.416	481.650	1.252	654.638	2.429	887.860	0.159
	0.2	0.5	23.475	0.235	35.222	0.168	45.208	0.082	50.202	0.643
		1	52.963	0.172	73.754	0.371	91.647	0.243	100.013	0.053
		1.5	82.280	0.055	112.580	0.245	137.792	0.175	150.032	0.122
		2	110.817	1.310	151.083	0.259	184.189	0.013	200.382	0.352
		2.5	140.504	0.360	189.712	0.248	231.015	1.019	250.026	0.039
		5	286.315	0.198	381.161	3.303	462.136	0.042	500.155	0.253
	0.3	0.5	19.676	0.112	28.020	0.029	32.434	0.013	33.351	0.013
		1	44.787	0.534	58.439	0.178	64.022	1.273	66.668	0.022
		1.5	69.095	0.077	88.851	0.046	96.815	1.719	100.637	0.725
		2	93.576	0.072	119.163	0.085	131.212	1.654	133.657	0.320
		2.5	118.018	0.747	149.359	0.152	164.591	0.013	166.754	0.098
		5	240.140	0.319	300.617	0.115	329.714	0.244	332.034	3.257
	0.4	0.5	16.638	0.062	22.754	0.017	24.676	0.692	25.022	0.017
		1	37.971	0.225	46.925	0.005	50.021	0.021	49.654	1.270
		1.5	58.701	0.015	71.157	0.390	74.992	0.400	75.179	0.371
		2	79.523	0.237	93.692	2.628	100.029	0.051	100.158	0.116
		2.5	100.142	0.006	118.822	0.031	125.184	0.308	125.028	0.027
		5	203.310	0.436	238.356	0.544	249.886	0.299	248.301	3.859

The analysis results suggest that when $kB/c_u < 2$, q_u is influenced by H/B, whereas for higher values of kB/c_u (2, 5, 10, and 20), H/B minimally influenced q_u. Hence, for each value of kB/c_u, $c_u/(\gamma B)$, and k_h, the values of q_u are presented for different H/B ratios in Table 5. In contrast, the values of q_u obtained for the different H/B values and each kB/c_u, $c_u/(\gamma B)$, and k_h are averaged in Table 6, and the standard deviation is presented.

5 Example

A 1 m width and perfectly rough strip footing is to be constructed 2 m away from an excavation at a height of 5 m. Design charts should be used to evaluate the bearing capacity of the strip footing. The undrained geotechnical conditions are as follows: c_u = 40 kPa, k = 400 kN/m^2/m, γ = 20 kN/m^3, k_h = 0.1.

Solution:

$$c_u/(\gamma B) = 40/(20\times 1) = 2,$$

$$kB/c_u = 400/40 = 10,$$

$$L/B = 2/1 = 2,$$

$$H/B = 5.$$

Using Fig. 7(d) and considering $c_u/(\gamma B) = 2$ and $kB/c_u = 10$ for $L/B = 2$ and $H/B = 5$,

$$q_u/(\gamma B) = 17.3.$$

Finally, the bearing capacity is obtained as $q_u = 17.3 \times 20 \times 1 = 346$ kPa.

6 Conclusions

Lower and upper bounds of the FELA were adopted to compute the undrained seismic bearing capacity of a strip footing sited close to a heterogeneous excavation. The effects of several variables, including the setback distance ratio (L/B), excavation height ratio (H/B), soil strength heterogeneity (kB/c_u), and horizontal earthquake coefficient (k_h), on the normalized bearing capacity ($q_u/(\gamma B)$) were evaluated. The conclusions of this study are as follows.

1) The results of the proposed method were compared with those of previous studies and demonstrated a good agreement.

2) The threshold value depends on kB/c_u, L/B, and H/B. However, the first two parameters had a more significant influence than the latter.

3) In all cases, $q_u/(\gamma B)$ increased with an increase in L/B and stabilized at a specific L/B value. Thus, an optimum distance exists from the excavation at which the footing can be placed safely because the bearing capacity is maximum and does not change at further distances.

4) kB/c_u significantly influenced the normalized bearing capacity. In contrast, H/B was the least influential variable on the bearing capacity.

5) An increase in k_h resulted in a decrease in the normalized bearing capacity. In addition, at a high horizontal earthquake coefficient, the effect of heterogeneity on the maximum bearing capacity disappears, indicating that both heterogeneous and homogenous soils have equal maximum bearing capacities.

References

1. Lyamin A V, Sloan S W. Lower bound limit analysis using non-linear programming. International Journal for Numerical Methods in Engineering, 2002, 55(5): 573−611
2. Lyamin A V, Sloan S W. Upper bound limit analysis using linear finite elements and non-linear programming. International Journal for Numerical and Analytical Methods in Geomechanics, 2002, 26(2): 181−216
3. Pastor J, Thai T H, Francescato P. New bounds for the height limit of a vertical slope. International Journal for Numerical and Analytical Methods in Geomechanics, 2000, 24(2): 165−182
4. Sloan S W. Geotechnical stability analysis. Geotechnique, 2013, 63(7): 531−571
5. Yu H S, Salgado R, Sloan S W, Kim J M. Limit analysis versus limit equilibrium for slope stability. Journal of Geotechnical and Geoenvironmental Engineering, 1998, 124(1): 1−11
6. Martin C M. The use of adaptive finite-element limit analysis to reveal slip-line fields. Géotechnique Letters, 2011, 1(2): 23−29
7. Ukritchon B, Yoang S, Keawsawasvong S. Undrained stability of unsupported rectangular excavations in non-homogeneous clays. Computers and Geotechnics, 2020, 117: 103281
8. Beygi M, Vali R, Porhoseini R, Keshavarz A, Maleksaeedi E. The effect of rotational stiffness on the behaviour of retaining wall. International Journal of Geotechnical Engineering, 2021, 15(7): 845−856
9. Shiau J S, Merifield R S, Lyamin A V, Sloan S W. Undrained stability of footings on slopes. International Journal of Geomechanics, 2011, 11(5): 381−390
10. Chen Q, Abu-Farsakh M. Ultimate bearing capacity analysis of strip footings on reinforced soil foundation. Soil and Foundation, 2015, 55(1): 74−85
11. Ghosh S, Debnath L. Seismic bearing capacity of shallow strip footing with Coulomb failure mechanism using limit equilibrium method. Geotechnical and Geological Engineering, 2017, 35(6): 2647−2661
12. Jadar C M, Ghosh S. Seismic bearing capacity of shallow strip footing using horizontal slice method. International Journal of Geotechnical Engineering, 2017, 11(1): 38−50
13. Veiskarami M, Jamshidi Chenari R, Jameei A A. Bearing capacity of strip footings on anisotropic soils by the finite elements and linear programming. International Journal of Geomechanics, 2017, 17(12): 04017119
14. Chavda J T, Dodagoudar G R. Finite element evaluation of ultimate capacity of strip footing: Assessment using various constitutive models and sensitivity analysis. Innovative Infrastructure Solutions, 2018, 3(1): 1−10
15. Vali R, Saberian M, Li J, Shams G, van Gelder P. Properties of geogrid-reinforced marine slope due to the groundwater level changes. Marine Georesources and Geotechnology, 2018, 36(6):

735−748

16. Kumar J, Mohan Rao V B K. Seismic bearing capacity of foundations on slopes. Geotechnique, 2003, 53(3): 347−361
17. Azzouz A S, Baligh M M. Loaded areas on cohesive slopes. Journal of Geotechnical Engineering, 1983, 109(5): 724−729
18. Graham J, Andrews M, Shields D H. Stress characteristics for shallow footings in cohesionless slopes. Canadian Geotechnical Journal, 1988, 25(2): 238−249
19. Shiau J S, Watson J F. 3D bearing capacity of shallow foundations located near deep excavation sites. In: Proceedings of the 2008 International Conference on Deep Excavation (ICDE 2008). Singapore: International Tunnelling and Underground Space Association (ITA), 2008
20. Georgiadis K. The influence of load inclination on the undrained bearing capacity of strip footings on slopes. Computers and Geotechnics, 2010, 37(3): 311−322
21. Georgiadis K. Undrained bearing capacity of strip footings on slopes. Journal of Geotechnical and Geoenvironmental Engineering, 2010, 136(5): 677−685
22. Salih Keskin M, Laman M. Model studies of bearing capacity of strip footing on sand slope. KSCE Journal of Civil Engineering, 2013, 17(4): 699−711
23. Vali R, Shams G, Porhoseini R, Saberian M, Beygi M. Lateral behaviour of pile located on top of a slope. Australian Geomechanics Journal, 2019, 54: 103−114
24. Mofidi Rouchi J, Farzaneh O, Askari F. Bearing capacity of strip footings near slopes using lower bound limit analysis. Civil Engineering Infrastructures Journal, 2014, 47: 89−109
25. Leshchinsky B, Xie Y. Bearing capacity for spread footings placed near $c'-\varphi'$ slopes Journal of Geotechnical and Geoenvironmental Engineering, 2017, 143(1): 06016020
26. Halder K, Chakraborty D, Kumar Dash S. Bearing capacity of a strip footing situated on soil slope using a non-associated flow rule in lower bound limit analysis. International Journal of Geotechnical Engineering, 2019, 13(2): 103−111
27. Zhou H, Zheng G, Yin X, Jia R, Yang X. The bearing capacity and failure mechanism of a vertically loaded strip footing placed on the top of slopes. Computers and Geotechnics, 2018, 94: 12−21
28. Jamshidi Chenari R, Kamyab Farahbakhsh H, Izadi A. Continuous slip surface method for stability analysis of heterogeneous vertical trenches. Scientia Iranica, 2020, 27(6): 2657−2668
29. Keshavarz A, Beygi M, Vali R. Undrained seismic bearing capacity of strip footing placed on homogeneous and heterogeneous soil slopes by finite element limit analysis. Computers and Geotechnics, 2019, 113: 103094
30. Gourvenec S M, Mana D S K. Undrained vertical bearing capacity factors for shallow foundations. Géotechnique Letters, 2011, 1(4): 101−108
31. Jamshidi Chenari R, Zhalehjoo N, Karimian A. Estimation on bearing capacity of shallow foundations in heterogeneous deposits using analytical and numerical methods. Scientia Iranica, 2014, 21: 505−515
32. Jamshidi Chenari R, Zamanzadeh M. Uncertainty assessment of critical excavation depth of vertical unsupported cuts in undrained clay using random feld theorem. Scientia Iranica, 2016, 23: 864−875
33. Sloan S W. Lower bound limit analysis using finite elements and linear programming. International Journal for Numerical and Analytical Methods in Geomechanics, 1988, 12(1): 61−77
34. Sloan S W. Upper bound limit analysis using finite elements and linear programming. International Journal for Numerical and Analytical Methods in Geomechanics, 1989, 13(3): 263−282
35. Foroutan Kalourazi A, Jamshidi Chenari R, Veiskarami M. Bearing capacity of strip footings adjacent to anisotropic slopes using the lower bound finite element method. International Journal of Geomechanics, 2020, 20(11): 04020213
36. Optum computational engineering (OptumG2). Copenhagen: Optum CE, 2015
37. Beygi M, Keshavarz A, Abbaspour M, Vali R, Saberian M, Li J. Finite element limit analysis of the seismic bearing capacity of strip footing adjacent to excavation in $c-\varphi$ soil Geomechanics and Geoengineering, 2022, 17(1): 246−259
38. Vali R, Foroughi Boroujeni F. Ground surface displacements and failure mechanisms induced by EPB shield tunneling method and groundwater levels changes. Transportation Infrastructure Geotechnology, 2022, 2022: 1−23
39. Vali R, Saberian M, Beygi M, Porhoseini R, Abbaspour M. Numerical analysis of laterally loaded single-pile behavior affected by urban metro tunnel. Indian Geotechnical Journal, 2020, 50(3): 410−425
40. Beygi M, Vali R, Keshavarz A. Pseudo-static bearing capacity of strip footing with vertical skirts resting on cohesionless slopes by finite element limit analysis. Geomechanics and Geoengineering, 2022, 17(2): 485−498
41. Vali R, Beygi M, Saberian M, Li J. Bearing capacity of ring foundation due to various loading positions by finite element limit analysis. Computers and Geotechnics, 2019, 110: 94−113
42. Izadi A, Foroutan Kalourazi A, Jamshidi Chenari R. Effect of roughness on seismic bearing capacity of shallow foundations near slopes using the lower bound finite element method. International Journal of Geomechanics, 2021, 21(3): 06020043
43. Beygi M, Keshavarz A, Abbaspour M, Vali R. 3D numerical study of the piled raft behaviour due to groundwater level changes in the frictional soil. International Journal of Geotechnical Engineering, 2020, 14(6): 665−672
44. Fathipour H, Payan M, Jamshidi Chenari R, Fatahi B. General failure envelope of eccentrically and obliquely loaded strip footings resting on an inherently anisotropic granular medium. Computers and Geotechnics, 2022, 146: 104734
45. Chen T, Xiao S. An upper bound solution to undrained bearing capacity of rigid strip footings near slopes. International Journal of Civil Engineering, 2020, 18(4): 475−485
46. Foroutan Kalourazi A, Izadi A, Jamshidi Chenari R. Seismic bearing capacity of shallow strip foundations in the vicinity of slopes using the lower bound finite element method. Soil and Foundation, 2019, 59(6): 1891−1905
47. Ukritchon B, Whittle A J, Klangvijit C. Calculations of bearing capacity factor N_γ using numerical limit analyses. Journal of Geotechnical and Geoenvironmental Engineering, 2003, 129(5): 468−474
48. Hjiaj M, Lyamin A V, Sloan S W. Numerical limit analysis solutions for the bearing capacity factor N_γ. International Journal of

Solids and Structures, 2005, 42(5−6): 1681−1704
49. Kumar J, Kouzer K M. Effect of footing roughness on bearing capacity factor N_γ. Journal of Geotechnical and Geoenvironmental Engineering, 2007, 133(5): 502−511
50. Kumar J. The variation of N_γ with footing roughness using the method of characteristics. International Journal for Numerical and Analytical Methods in Geomechanics, 2009, 33(2): 275−284
51. Kumar J, Chakraborty D. Seismic bearing capacity of foundations on cohesionless slopes. Journal of Geotechnical and Geoenvironmental Engineering, 2013, 139(11): 1986−1993
52. Pakdel P, Jamshidi Chenari R, Veiskarami M. An estimate of the bearing capacity of shallow foundations on anisotropic soil by limit equilibrium and soft computing technique. Geomechanics and Geoengineering, 2019, 14(3): 202−217